Dependence of adsorption-induced structural transition on framework structure of porous coordination polymers

Ryohei Numaguchi, Hideki Tanaka, Satoshi Watanabe, and Minoru T. Miyahara

Articles you may be interested in

Simulation study for adsorption-induced structural transition in stacked-layer porous coordination polymers: Equilibrium and hysteretic adsorption behaviors
J. Chem. Phys. **138**, 054708 (2013); 10.1063/1.4789810

Understanding adsorption-induced structural transitions in metal-organic frameworks: From the unit cell to the crystal
J. Chem. Phys. **137**, 184702 (2012); 10.1063/1.4765369

Free energy landscapes for the thermodynamic understanding of adsorption-induced deformations and structural transitions in porous materials
J. Chem. Phys. **137**, 044118 (2012); 10.1063/1.4738776

Osmotic ensemble methods for predicting adsorption-induced structural transitions in nanoporous materials using molecular simulations
J. Chem. Phys. **134**, 184103 (2011); 10.1063/1.3586807

Free energy analysis for adsorption-induced lattice transition of flexible coordination framework
J. Chem. Phys. **130**, 164707 (2009); 10.1063/1.3122988

Dependence of adsorption-induced structural transition on framework structure of porous coordination polymers

Ryohei Numaguchi, Hideki Tanaka, Satoshi Watanabe, and Minoru T. Miyahara[a)]
Department of Chemical Engineering, Kyoto University, Katsura, Nishikyo, Kyoto 615-8510, Japan

Porous coordination polymers (PCPs) with soft frameworks show a gate phenomenon consisting of an abrupt structural transition induced by adsorption of guest molecules. To understand the dependence of the gating behavior on the host framework structure, we conduct grand canonical Monte Carlo simulations and a free-energy analysis of a simplified model of a stacked-layer PCP. The interlayer width of the rigid layers composing the simplified model can be changed by guest adsorption and by varying the initial interlayer width h_0, which is controlled by the length of pillars between the layers. We introduce three types of gating behavior, one-step gating, filling and gating, and double gating, which depend on three parameters: the initial interlayer width h_0; the interaction parameter ε_{ss}, which determines the host–guest framework interaction as well as the inter-framework interaction; and the elastic modulus of the framework, which depends on the stiffness of the pillars. We show that the one-step gating and the filling and gating behaviors depend strongly on h_0 rather than on ε_{ss}, and thus a transformation from filling and gating to double gating can be achieved by reducing the stiffness of the host framework. This study should be a guideline for controlling the gating pressure of PCPs by modifying their chemical components. © *2014 AIP Publishing LLC*. [http://dx.doi.org/10.1063/1.4862735]

I. INTRODUCTION

There is a growing interest in novel porous materials, commonly called porous coordination polymers (PCPs) and metal–organic frameworks (MOFs).[1–3] PCPs have highly ordered structures composed of metal cations, counteranions, and organic linkers, which allow tailoring of the pore size and inner pore functionality. In addition, PCPs with "soft" frameworks (soft PCPs) show a peculiar adsorption behavior accompanied by a structural transition of the framework, the so-called gate phenomenon or breathing phenomenon.[4] The gate phenomenon involves a stepwise increase in the number of adsorbed guest molecules with a dramatic deformation of the host framework which increases in pore volume at a certain pressure (gate opening), and abrupt desorption with restoration of the host structure at a lower pressure than the gate-opening pressure (gate closing). This phenomenon has been reported for several soft PCP motifs, e.g., one-dimensional channels,[5] two-dimensional stacked layers,[6–11] and three-dimensional interpenetrating motifs.[12–14] The breathing phenomenon, which is typically observed for MIL-53 family,[15–20] consists of abrupt shrinkage of the host structure followed by expansion upon adsorption. The soft PCPs have shown different structural transition behaviors, which could be suitable for various applications such as gas storage,[7,21] separation,[9] and molecular sensing;[22] however, for their application in industry, precise control of the structural transition behavior is required. One method of regulating it is to tune the components of the soft PCP while keeping its original morphology. Férey *et al.* synthesized soft PCPs, MIL-53(Cr)[20] and MIL-

53(Al),[23] with different metal species that have similar crystal structures. MIL-53(Al) showed a structural transition induced by CO_2 adsorption at a 30% higher pressure than that of MIL-53(Cr).[19] Various PCPs were also synthesized by changing the organic ligand[24,25] and the counteranion,[6,26] and the gate-opening and/or gate-closing pressures were successfully tuned by 10% to 100%. On the other hand, a dramatic change in the shape of the adsorption isotherm was reported in some component-tuned PCPs, although the tuning retained the morphology of the host structure. For example, MIL-53 materials with metal species such as Fe^{3+}, Ga^{3+}, and Sc^{3+} have more shrunk structure than MIL-53(Al) and MIL-53(Cr) in the degassed state, and show totally different structural transition behavior from the typical breathing phenomenon.[15–18,27] Moreover, ELM-11[8] and ELM-12,[26] which have similar crystal morphologies and chemical components except for the counteranion, have a different number of stepwise uptakes in their N_2 adsorption isotherms: ELM-11 shows a step in the adsorption isotherm, which is attributed to an adsorption-induced structural transition from the non-porous degassed structure to the N_2-adsorbed one. On the other hand, ELM-12 exhibits two steps in the adsorption isotherm, which come from micropore filling in a porous degassed structure and subsequent gate adsorption. The latter "filling and gating" adsorption was also observed for amine-functionalized MIL-53.[24] Moreover, the gating behavior can be more finely controlled by making a solid solution of two parental PCPs with similar crystal structures.[25,28,29] The solid-solution PCP shows an intermediate adsorption isotherm between those of the parental PCPs, and the gate-opening and -closing pressures can be tuned continuously by varying the ratio of the parental PCPs. More interestingly, a phase-separated PCP[28]

a)Author to whom correspondence should be addressed. Electronic mail: miyahara@cheme.kyoto-u.ac.jp

consisting of the inner crystal of one parental PCP and the outer crystal of the other parental PCP exhibits a different adsorption isotherm from that of the solid-solution PCP with the same chemical formula. This indicates that the mesoscopic design of the PCP can change the gating behavior. The crystal size of the PCP can also be a parameter for controlling the gating behavior.[30,31] The adsorption isotherm of the PCP nanocrystals shows a 50% higher gate-opening pressure with more gradual uptake than that of the bulk micrometer-sized crystals.

Molecular simulations have provided a useful microscopic insight for understanding the adsorption behavior of gases on PCPs. Grand canonical Monte Carlo (GCMC) simulations were conducted to evaluate the gas adsorption[32–36] and separation[37–42] capacities of PCPs. The diffusivities of guest molecules in PCPs were investigated by molecular dynamics (MD) simulations.[34,35,43,44] Then, a large-scale computational screening of PCPs for gas storage and separation was recently performed on the basis of the MD and GCMC simulations.[45,46] These simulation studies used a PCP model with a rigid framework; however, several simulation studies indicated the importance of taking into account the flexibility of the PCP framework. For example, the negative thermal expansion,[47,48] thermal conductivity,[49] and conformational isomerization[50] of the PCP frameworks were very recently reproduced with flexible framework models. Then, the diffusion of guest molecules in the flexible PCP model was investigated by an MD simulation by Amirjalayer *et al.*,[51] who revealed that the self-diffusion coefficient is smaller than that calculated with the rigid PCP model. Regarding the gating behavior of soft PCPs, Maurin *et al.*[52–54] simulated the CO_2 adsorption on MIL-53 by a hybrid osmotic Monte Carlo method, in which trials of the insertion and deletion of the guest molecule and the deformation of the host were performed. The structural transition of MIL-53 from a large-pore (*lp*) state to a narrow-pore (*np*) state was successfully simulated by their method, but abrupt expansion from the *np* state to the *lp* state at a higher pressure cannot be achieved because of the difficulty in sampling the full phase space. To avoid this difficulty, Triguero *et al.*[55,56] constructed a simplified model of MIL-53 taking into account the layer-by-layer shear to the crystal and succeeded in direct simulation of the structural transition behavior. Their results suggested that the spontaneous structural transition pressures depend on the long-range elastic cell–cell interaction, which penalizes the formation of an interface between two crystal phases with the *lp* and *np* structures. Free-energy analysis is another method of addressing the difficulty with direct simulation of the gating behavior. The free energy landscape as a function of the deformation of the host framework structure and the chemical potential of the guest molecule can be calculated by a combination of a GCMC simulation and a thermodynamic integration method. A stable state is determined by exploring a global minimum in the landscape. This method was applied to simplified models of PCPs with the mutually interpenetrating,[57,58] stacked-layer,[59] and one-dimensional lozenge-shape channel (breathing) motifs.[60,61] These studies revealed that the adsorption-induced structural transition occurs when an energy penalty for the host deformation is surmounted by stabilization due

to the adsorption of the guest molecules, and that a difference in energy barriers between the pre- and post-transition states for the adsorption and desorption processes causes adsorption hysteresis. The dependence of the gating behavior on the framework structure of the interpenetrated PCP was first demonstrated by Watanabe *et al.*[58] They constructed two models composed of intersecting rods with different thicknesses and fluid–frame and inter-framework interactions. The difference in the rod thickness, which corresponds to a change in the organic linker of the PCP, resulted in different gating behavior (i.e., one-step gating for the thick-rod model and filling and gating for the thin-rod model) because the thin-rod model provides a space to accommodate the guest molecules in a degassed state, whereas the thick-rod model has a non-porous degassed state. Very recently, Bousquet *et al.*[61] examined the structural transition behavior of a simple model of MIL-53 under thermodynamic equilibrium. They revealed that the structural transition behavior is dramatically changed by arbitrarily varying the Helmholtz free energy profile of the host framework and Henry's constant depending on the size of the guest molecule. However, in these studies, the effects of the change in the chemical components of the PCP on the structural transition pressure are still not fully understood.

In this study, we report the dependence of the gating behavior on the framework structure of the simplified stacked-layer PCP model used in a previous study,[59] which can be characterized by two parameters: the initial interlayer width h_0 and interlayer interaction parameter ε_{ss} based on the Lennard–Jones (LJ) potential. The equilibrium structural transition pressure and the spontaneous gate-opening and -closing pressures are determined by the GCMC simulation and a free-energy analysis. The dependence of the one-step gating behavior on h_0 at fixed ε_{ss} and on ε_{ss} at fixed h_0 is demonstrated. Then, the parameter sets of h_0 and ε_{ss} that provide one-step gating behavior are explored. The models showing filling and gating behavior are also determined by tuning the parameter sets, revealing how the change in the parameters produces a dramatic change in the gating behavior. We also examine the gating behavior of a PCP model that has virtual springs between the layers in order to discuss the correlation between the elasticity of the host and the gating behavior. This study should serve as a guideline for tuning the gating pressure and controlling the shape of the adsorption isotherm by modifying the PCP components.

II. METHODS

A. Simulation models and details

To model the stacked-layer PCP, we constructed a simplified model, depicted in Fig. 1, which is the same as that used in our previous study.[59] The model consists of rigid smeared-atom layers and pillaring atoms located on one side of the layers. The interlayer widths for all the neighboring layers, h, were assumed to remain the same when the system was deformed by guest adsorption and desorption. The 12-6 LJ potential was used to describe the fluid–fluid interaction u^{ff}, and the potential parameters used were those of argon: $\sigma_{ff} = 0.341$ nm and $\varepsilon_{ff}/k_B = 119.8$ K, where k_B is the
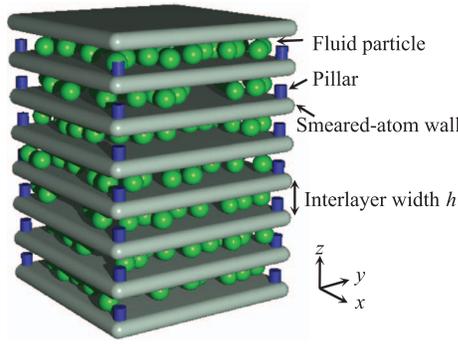
FIG. 1. Schematic illustration of simplified stacked-layer PCP model.

Boltzmann constant. Then, the 10-4 LJ potential was used for fluid–solid interaction u^{fs}:

$$u^{fs}(z_{ik}) = 2\pi \rho_s \varepsilon_{fs} \sigma_{fs}^2 \left\{ \frac{2}{5} \left(\frac{\sigma_{fs}}{z_{ik}} \right)^{10} - \left(\frac{\sigma_{fs}}{z_{ik}} \right)^4 \right\}, \quad (1)$$

where z_{ik} denotes the distance between the ith fluid molecule and the kth layer, and ρ_s is the atomic number density of the layer, which was set to $2.2/\sigma_{ff}^2$. The solid–fluid parameters, ε_{fs} and σ_{fs}, were calculated according to the Lorentz–Berthelot mixing rules. Then, the layer–layer interaction u^{ll} was derived from the area integral of the 10-4 LJ potential as

$$u^{ll}(h_{kl}) = 2\pi \rho_s^2 \varepsilon_{ss} \sigma_{ss}^2 \left\{ \frac{2}{5} \left(\frac{\sigma_{ss}}{h_{kl}} \right)^{10} - \left(\frac{\sigma_{ss}}{h_{kl}} \right)^4 \right\}, \quad (2)$$

where ε_{ss} and σ_{ss} are the interlayer LJ parameters, and h_{kl} is the distance, $(k - l)h$, between the kth and lth layers. The σ_{ss} value was set to 0.34 nm, and ε_{ss}/k_B was varied from 5 K to 300 K in this study. The layer–pillar interaction u^{lp} and pillar–pillar interaction u^{pp} were calculated using the 10-4 LJ and 12-6 LJ potentials, respectively. The LJ parameters of the pillar were the same as those of the guest molecule, and the density of the pillar was set to $1/(100\sigma_{ff}^2)$. Interactions between the pillars and the guest molecules were neglected because of the low density of the pillars. All the potentials were cut and shifted at a distance of $5\sigma_{ff}$. The total potential of the host framework U^{ss} is expressed as

$$U^{ss} = \sum_{k=1}^{N_L-1} \sum_{l=k+1}^{N_L} u^{ll}(h_{kl}) + \sum_{k=1}^{N_L} \sum_{l=1, \neq k}^{N_L} u^{lp}(h_{kl} + d_p)$$
$$+ \sum_{k=1}^{N_L-1} \sum_{l=k+1}^{N_L} u^{pp}(r_{kl}), \quad (3)$$

where N_L is the number of the layers in the system, d_p is the distance from a layer to the attached pillar, and r_{kl} is the pillar–pillar distance (see Fig. S1 in the supplementary material[62] for a graphic explanation of Eq. (3)). The initial interlayer width h_0 at which U^{ss} has the minimum value was varied from $1.25\sigma_{ff}$ to $3.00\sigma_{ff}$ by tuning the pillar length d_p. Actually, electrostatic interactions should contribute to the interaction potential of the host, U^{ss}, for a real PCP, but the contribution may be approximately reproduced by tuning ε_{ss} as mentioned above. Hence, the electrostatic interactions were not considered in our model for the sake of simplicity. The simulation

cell was composed of stacked unit cells (uc) which contain one layer and an interlayer space. The size of the unit cell was $10\sigma_{ff} \times 10\sigma_{ff}$ in the x–y layer direction and $1.20\sigma_{ff}$–$2.70\sigma_{ff}$ in the z direction normal to the layers. The number of stacked unit cells was determined so that the z length of the simulation cell was larger than $10\sigma_{ff}$. Periodic boundary conditions were imposed for all the directions. The relation between the chemical potential of the system and the bulk fluid pressure was obtained by the Johnson–Zollweg–Gubbins equation of state.[63] The saturated vapor pressure of the LJ fluid obtained by Lotfi *et al.*[64] was used to calculate the relative pressure P/P_0.

GCMC simulations were conducted to obtain the adsorption isotherm of argon in the simplified stacked-layer PCP models. The length of the simulation run was at least 2.5×10^7 steps for equilibration and 2×10^8 steps for sampling. The reduced temperature of the system, $k_B T/\varepsilon_{ff}$, was set to 0.8 for all the cases in this study.

B. Free-energy calculation

The osmotic free energy of the system Ω^{OS} was calculated by the following equation:[65]

$$\Omega^{OS}(\mu, h) = F^{host}(h) + PV(h) + \Omega(\mu, h), \quad (4)$$

where F^{host} is the Helmholtz free energy of the host, P is the bulk pressure, $V(h)$ is the system volume at the interlayer width h, and Ω indicates the grand free energy of the guest molecules adsorbed on the system with a fixed h, which can be calculated by thermodynamic integration of the adsorption isotherm, $N(\mu, h)$, as a function of the chemical potential of the fluid μ:[66]

$$\Omega(\mu, h) = - \int_{-\infty}^{\mu} N(\mu, h) \, d\mu. \quad (5)$$

Then, the relative osmotic free energy $\Delta \Omega^{OS}$ is defined as

$$\Delta \Omega^{OS}(\mu, h) = \Omega^{OS}(\mu, h) - \Omega^{OS}(\mu, h_0)$$
$$= \Delta F^{host} + P\Delta V(h) + \Delta \Omega(\mu, h), \quad (6)$$

where ΔV and $\Delta \Omega$ are the changes in the volume and grand free energy of the system, respectively. The relative Helmholtz energy of the host, $\Delta F^{host}(h) = F^{host}(h) - F^{host}(h_0)$, was approximated by the difference in the interlayer potential, $\Delta U^{ss}(h) = U^{ss}(h) - U^{ss}(h_0)$. This approximation can be reasonable in our model because the thermal fluctuation of the layer itself will change very little with variations in the interlayer width, so the entropy change in $\Delta F^{host}(h)$ can be negligible.

III. RESULTS AND DISCUSSION

A. Dependence of one-step gating behavior on initial interlayer width h_0

Figure 2(a) shows the relative free energies as a function of the interlayer width for the model with $h_0/\sigma_{ff} = 1.85$ and $\varepsilon_{ss}/k_B = 28$ K at a relative pressure of $P/P_0 = 0.007$. The relative Helmholtz free energy of the host, ΔF^{host}, which is independent of the gas pressure, has a single minimum at
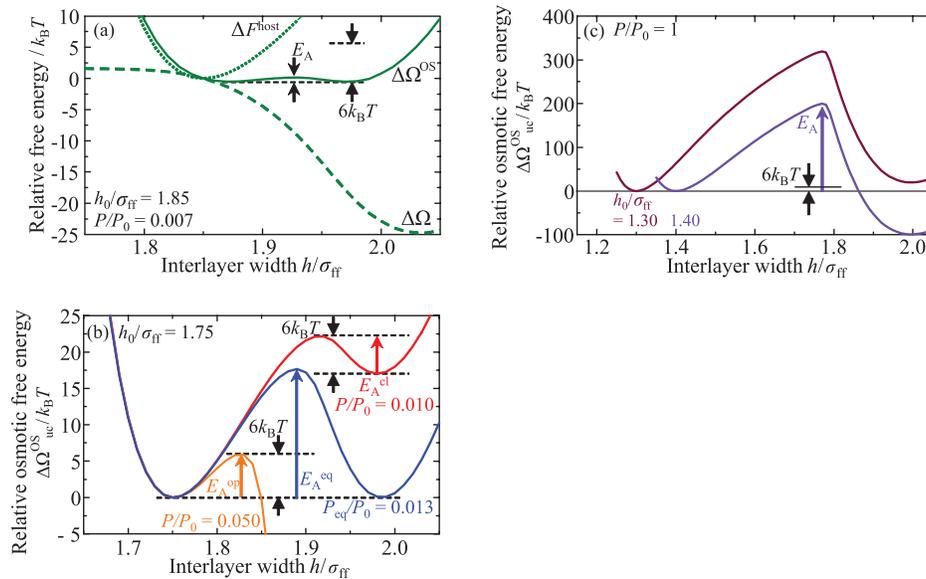
FIG. 2. (a) Relative free energies $\Delta\Omega^{OS}$, $\Delta\Omega$, and ΔF^{host} for the model with $h_0/\sigma_{ff} = 1.85$ as a function of the interlayer width at $P/P_0 = 0.007$; (b) relative osmotic free energies for the model with $h_0/\sigma_{ff} = 1.75$ at $P/P_0 = 0.010$, 0.013, and 0.050; (c) relative osmotic free energies for the models with $h_0/\sigma_{ff} = 1.30$ and 1.40 at $P/P_0 = 1$. An interaction parameter ε_{ss}/k_B of 28 K was used for all the models.

$h = h_0$ (degassed state), and it increases monotonically as the interlayer width h increases, because the layers are drawn apart against the interlayer attractive force. The relative grand free energy of the guest, $\Delta\Omega$, decreases with increasing h and has a minimum at $h_0/\sigma_{ff} = 2.03$, where the guest molecules are the most stably accommodated. The relative osmotic free energy $\Delta\Omega^{OS}$ was calculated as the sum of the ΔF^{host}, $\Delta\Omega$, and $P\Delta V$ terms according to Eq. (6). The profile of $\Delta\Omega^{OS}$ becomes bistable at $P/P_0 = 0.007$, indicating that a closed state ($h/\sigma_{ff} = 1.87$) and an open state ($h/\sigma_{ff} = 1.97$) are in thermodynamic equilibrium. An energy barrier, $E_A^{eq} = 0.64\ k_BT/uc$, appears between the two stable states, and it depends on the magnitude of the energy fluctuation of the system whether the system can overcome the energy barrier or not. The energy barrier and the energy fluctuation of the system are system-size dependent, and therefore we assumed that a huge PCP crystal was composed of small domains. In the previous study,[59] we showed that, according to the transition state theory, the energy fluctuation of the domain should be $35\ k_BT$ so that we observe the structural transition within 1 h for the domain of $8.3 \times 8.3 \times h = 43$ nm^3 (where h is the interlayer width of 0.62 nm in the activation state). The obtained energy fluctuation of $35\ k_BT$ is equivalent to $6\ k_BT/uc$ in this study. If we apply $6\ k_BT/uc$ as the system energy fluctuation for the model with $h_0/\sigma_{ff} = 1.85$, the structural transition should be observed at $P/P_0 = 0.007$ (hereafter, the equilibrium transition pressure) because $E_A^{eq} < 6\ k_BT/uc$. In this case, a reversible adsorption isotherm with a single step is obtained, as shown in Fig. 3(a). Then, if we set the initial interlayer width to $h_0/\sigma_{ff} = 1.75$, the bistable state is observed at $P/P_0 = 0.013$ (Fig. 2(b)). However, the equilibrium structural transition from the closed state ($h/\sigma_{ff} = 1.75$) to the open state ($h/\sigma_{ff} = 1.99$) should not occur because the energy barrier E_A^{eq} is higher than the system energy fluctuation of $6\ k_BT/uc$.

As the pressure increases from $P/P_0 = 0.013$, the global minimum switches from the closed state to the open state, and the energy barrier required for the structural transition toward the open state decreases owing to the stabilization by guest adsorption. The energy barrier E_A^{op} finally reaches $6\ k_BT/uc$ at $P/P_0 = 0.050$, and spontaneous gate opening can be observed. For the desorption process, the system stays at the open state down to $P/P_0 = 0.010$, where the energy barrier E_A^{cl} required for the transition from the open state to the closed state coincides with $6\ k_BT/uc$. Further decreases in the pressure reduce E_A^{cl} and trigger spontaneous gate closing. This is the mechanism of gate opening and closing with accompanying adsorption hysteresis; the resulting adsorption isotherm is shown in Fig. 3(b). If the initial interlayer width is further decreased to $h_0/\sigma_{ff} = 1.40$, E_A^{op} becomes larger than $6\ k_BT/uc$ even at
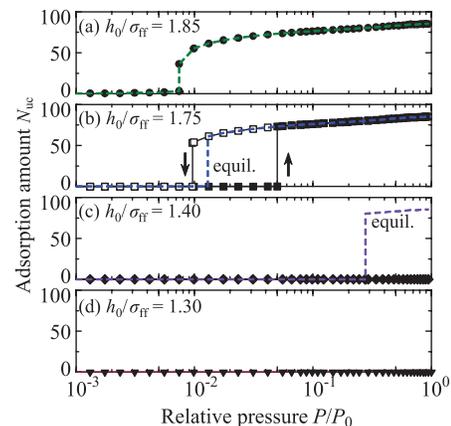
FIG. 3. Adsorption isotherms of models with initial interlayer widths h_0/σ_{ff} of (a) 1.85, (b) 1.75, (c) 1.40, and (d) 1.30. Filled and open symbols indicate adsorption and desorption isotherms, respectively. Dashed lines are adsorption isotherms at thermodynamic equilibrium. An interaction parameter ε_{ss}/k_B of 28 K was used for all the models.
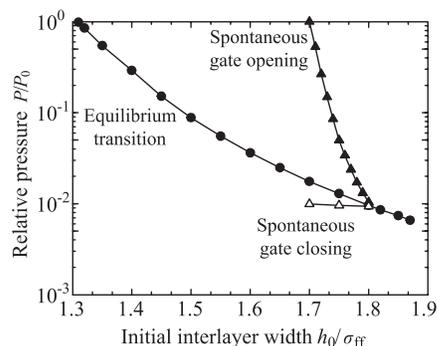
FIG. 4. Dependence of equilibrium and spontaneous gate-opening and -closing pressures on initial interlayer width h_0.

FIG. 5. (a) Relative osmotic free energies for models with $\varepsilon_{ss}/k_B = 7$ K and $h/\sigma_{ff} = 2.03$, $\varepsilon_{ss}/k_B = 14$ K and $h/\sigma_{ff} = 2.02$, and $\varepsilon_{ss}/k_B = 35$ K and $h/\sigma_{ff} = 1.99$ as a function of relative pressure; (b) adsorption isotherms of the three models. The initial interlayer width for all the models is $h_0/\sigma_{ff} = 1.70$.

$P/P_0 = 1$, although the global minimum switches from the closed state to the open state ($h/\sigma_{ff} = 1.99$) at a higher pressure than $P/P_0 = 0.277$ (Fig. 2(c)). Namely, according to the kinetics, the amount of adsorption for the model with $h_0/\sigma_{ff} = 1.40$ must be zero up to $P/P_0 = 1$, and a stepped adsorption isotherm is obtained according to the theory of equilibrium (Fig. 3(c)). Then, for $h_0/\sigma_{ff} = 1.30$, the global minimum does not switch from the closed state to the open state below $P/P_0 = 1$ (Fig. 2(c)); thus, adsorption of guest molecules is definitely not observed (Fig. 3(d)).

The dependence of the equilibrium transition pressure and spontaneous gate-opening and -closing pressures on the initial interlayer width h_0 is summarized in Fig. 4. The equilibrium transition pressure decreases with increasing h_0. This is because the work required to expand the interlayer spacing against the interlayer attractive force, which is equal to ΔF^{host}, becomes smaller as h_0 increases. Then, at $h_0/\sigma_{ff} = 1.87$, E_A^{eq} becomes zero (the $\Delta\Omega^{OS}$ profile always has a single minimum); therefore, the first-order equilibrium transition disappears. Spontaneous gate opening occurs at $P/P_0 = 1$ for the model with $h_0/\sigma_{ff} = 1.70$, assuming a system energy fluctuation of 6 $k_B T$/uc. The gate-opening pressure decreases sharply with increasing h_0/σ_{ff}, and it coincides with the equilibrium transition pressure at $h_0/\sigma_{ff} = 1.80$. The gate-closing pressure was determined for the models with initial interlayer widths larger than 1.70 because the gate-opening transition can be achieved for those models only below $P/P_0 = 1$. The gate-closing pressure is nearly independent of h_0 because the interlayer width h at the metastable open state before gate closing becomes almost the same among the models with different h_0 (see Fig. S2(a) in the supplementary material[62]). As in the gate-opening transition, the gate-closing pressure is consistent with the equilibrium transition pressure at $h_0/\sigma_{ff} = 1.80$. For the models with initial interlayer widths larger than 1.80, E_A^{eq} as well as E_A^{op} and E_A^{cl} become smaller than 6 $k_B T$/uc, which yields a reversible adsorption isotherm with a single step.

To summarize this section: with increasing h_0, the equilibrium transition pressure decreases, and the spontaneous gate-opening pressure sharply decreases, although the gate-closing pressure has a weak dependence, and this results in narrowing and disappearance of the hysteresis loop.
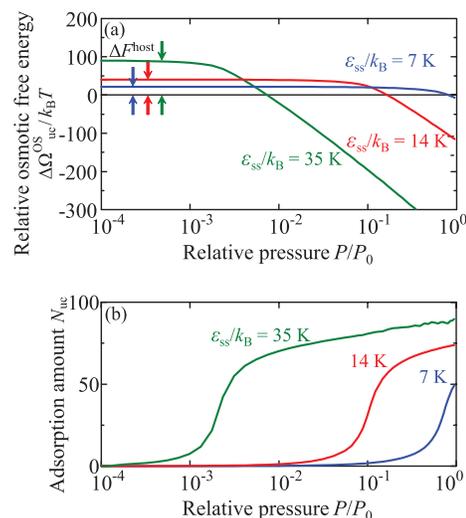
B. Dependence of one-step gating behavior on interaction parameter ε_{ss}

Tuning of the chemical components in real PCPs affects not only the geometrical configuration of the host framework but also the host–guest interaction and inter-framework interaction. This can be reproduced by changing the interaction parameter ε_{ss} in our model. Figure 5(a) shows the relative osmotic free energies for models with $\varepsilon_{ss}/k_B = 7$ K and $h/\sigma_{ff} = 2.03$, $\varepsilon_{ss}/k_B = 14$ K and $h/\sigma_{ff} = 2.02$, and $\varepsilon_{ss}/k_B = 35$ K and $h/\sigma_{ff} = 1.99$, calculated from the thermodynamic integration of the adsorption isotherms (Fig. 5(b)) as a function of the relative pressure. The interlayer widths h for the three models were fixed during the calculation, although each model has the same initial interlayer width of $h_0/\sigma_{ff} = 1.70$. The free-energy profile exhibits a plateau in the low-pressure region, and the height of the plateau, which corresponds to ΔF^{host}, is proportional to the magnitude of ε_{ss}. The relative osmotic free energy starts to decrease at the same time as the adsorption amount begins to increase with increasing pressure. The pressure at which $\Delta\Omega^{OS} = 0$ is where the equilibrium structural transition should occur. With increasing ε_{ss}, the equilibrium transition pressure decreases; nevertheless, the ΔF^{host} value required to deform the host framework is increased. This is because the increase in ε_{ss} enhances the host–guest interaction according to the Lorentz–Berthelot mixing rules.

Figure 6 shows the dependence of the equilibrium transition pressure and spontaneous gate-opening and -closing pressures on ε_{ss}. When the initial interlayer width h_0/σ_{ff} was set to 1.70, the models with $\varepsilon_{ss}/k_B < 5$ K cannot adsorb sufficient guest molecules to stabilize the deformed host framework owing to their weak host–guest interaction; therefore, the equilibrium structural transition should not be observed. Then, as ε_{ss}/k_B increases from 5 K, the equilibrium transition pressure decreases because the increase in ε_{ss} contributes greatly to the stabilization of the system by strengthening the host–guest interaction compared with the destabilization by the increase
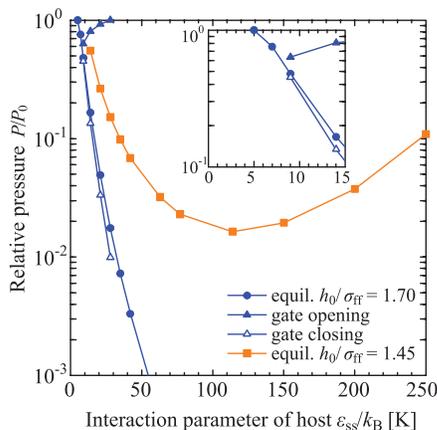
FIG. 6. Dependence of equilibrium and gate-opening and -closing transition pressures on interaction parameter ε_{ss} for models with $h_0/\sigma_{ff} = 1.45$ and 1.70.

in ΔF^{host}. The dependence on ε_{ss} for the model with $h_0/\sigma_{ff} = 1.45$, which has a larger ΔF^{host} than the model with $h_0/\sigma_{ff} = 1.70$, is also shown in Fig. 6 for comparison. The equilibrium transition pressure for the model with $h_0/\sigma_{ff} = 1.45$ shows a minimum at $\varepsilon_{ss}/k_B = 114$ K and begins to increase with increasing ε_{ss}. This is because the host–guest interaction parameter ε_{fs} is proportional to the square root of ε_{ss}; on the other hand, ΔF^{host} increases directly with ε_{ss}. Namely, the destabilization of the system by the increase in ΔF^{host} becomes significant over $\varepsilon_{ss}/k_B = 114$ K. Values of ε_{ss}/k_B larger than 9 K yield a hysteresis loop for the models with $h_0/\sigma_{ff} = 1.70$. The increase in ε_{ss} raises the gate-opening pressure as a consequence of the increase in the energy barrier. On the other hand, the gate-closing pressure sharply decreases with increasing ε_{ss}, which differs from the dependence on h_0. This is clear from the fact that desorption of guest molecules from

the model with a stronger host–guest interaction requires a greater reduction in the bulk gas pressure. These results suggest that the enhancement of the ε_{ss} value widens the hysteresis loop. As for the model with $h_0/\sigma_{ff} = 1.45$, no spontaneous transitions should be observed because E_A^{op} and E_A^{cl} are always larger than $6\,k_BT/\text{uc}$.

C. Parameter sets for one-step gating behavior

We explored the models showing the one-step gating behavior among the parameter sets of the initial interlayer width h_0 and interaction parameter ε_{ss}. We categorized the parameter sets into types (i)–(v); the results are summarized in Fig. 7(a). In area (i), which is blank, no structural transitions are observed because the global minimum of the osmotic free energy remains in the closed state even at $P/P_0 = 1$ (see Fig. 7(b) (i)). Then, the global minimum can switch from the closed state to the open state in areas (ii), (iii), and (iv) below $P/P_0 = 1$ (Figs. 7(b) (ii), 7(b) (iii), and 7(b) (iv), respectively). Therefore, according to the theory of equilibrium, a stepped adsorption isotherm is obtained in areas (ii), (iii), and (iv). In area (ii), E_A^{eq} is always larger than $6\,k_BT/\text{uc}$, and it follows that the structural transition does not occur according to the kinetics. In area (iii), spontaneous gate-opening and -closing transitions are observed on the basis of the kinetics because E_A^{op} and E_A^{cl} can become smaller than $6\,k_BT/\text{uc}$, although $E_A^{eq} > 6\,k_BT/\text{uc}$, below $P/P_0 = 1$ (Fig. 7(b) (iii)). In area (iv), even E_A^{eq} can be less than $6\,k_BT/\text{uc}$ (Fig. 7(b) (iv)), which yields a reversible adsorption isotherm with a single step. Then, in area (v), which is blank, the $\Delta\Omega^{OS}$ profile has a single minimum (Fig. 7(b) (v)), so the first-order equilibrium transition vanishes. The typical $\Delta\Omega^{OS}$ profiles at the borders between the areas are shown in the supplementary material (Fig. S3).[62] It is noteworthy that Bousquet *et al.*[61] have shown
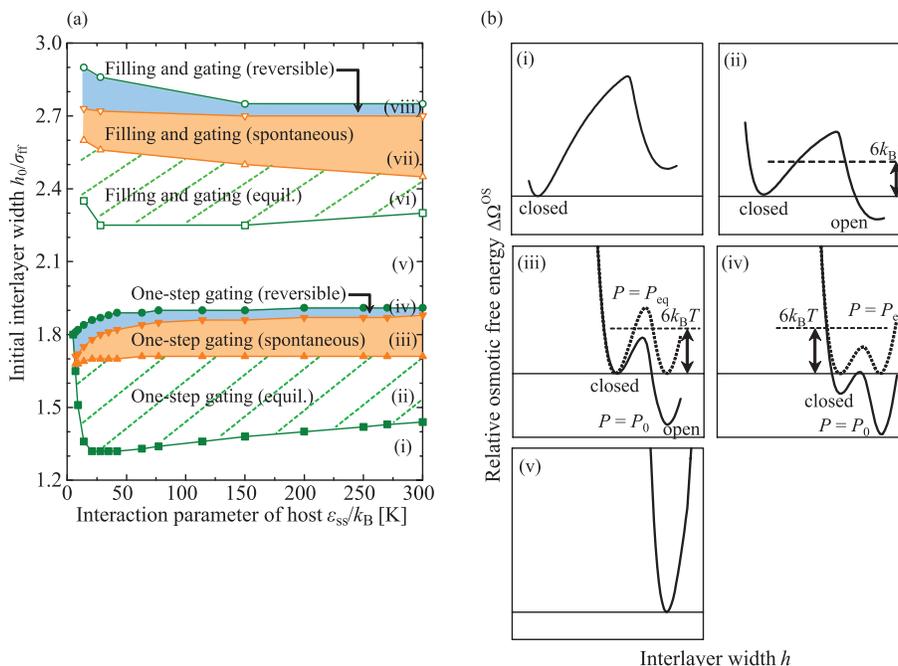
FIG. 7. (a) Parameter sets of host framework showing one-step gating and filling and gating behaviors observed below $P/P_0 = 1$; (b) schematic of typical relative osmotic free energies in areas (i)–(v) shown in (a).
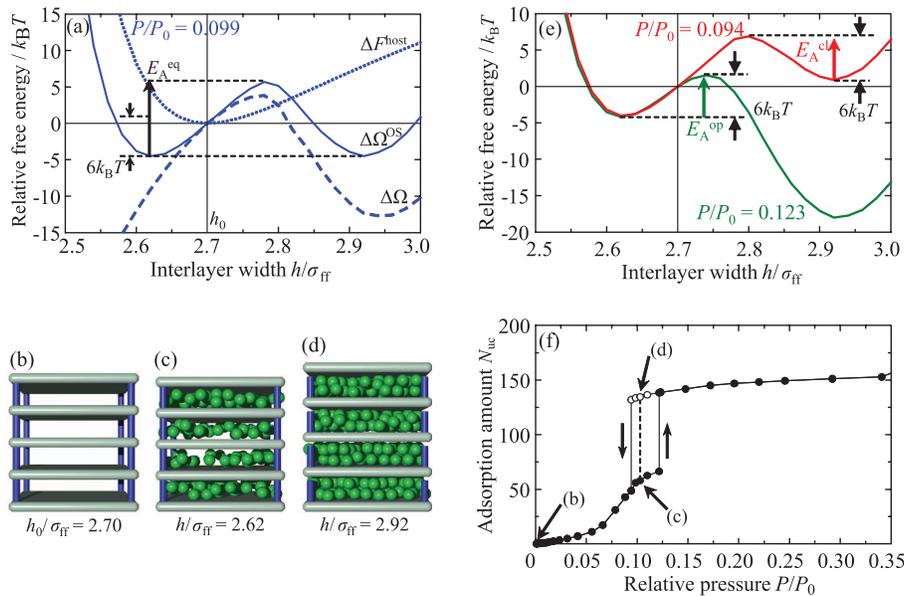
FIG. 8. (a) Relative free energies $\Delta\Omega^{OS}$, $\Delta\Omega$, and ΔF^{host} for model with $h_0/\sigma_{ff} = 2.70$ and $\varepsilon_{ss}/k_B = 28$ K as a function of interlayer width at $P/P_0 = 0.099$; snapshots of the system: (b) $h_0/\sigma_{ff} = 2.70$ and $P/P_0 = 0$, (c) $h/\sigma_{ff} = 2.62$ and $P/P_0 = 0.099$, and (d) $h/\sigma_{ff} = 2.92$ and $P/P_0 = 0.099$; (e) relative osmotic free energies at $P/P_0 = 0.094$ and $P/P_0 = 0.123$; (f) resulting adsorption isotherm.

that the first-order equilibrium transition vanishes in their simple model for MIL-53 with increasing the relative pore size to adsorbate (the change from Case 2 to Case 1 in Sec. II C).

Figure 7(a) shows that the border between areas (i) and (ii) strongly depends on ε_{ss}. The border has a minimum at $\varepsilon_{ss}/k_B = 28$ K, which is attributed to the difference in the dependence of ΔF^{host} and $\Delta\Omega$ on ε_{ss}; i.e., ΔF^{host} increases directly with ε_{ss}, whereas $\Delta\Omega$ is proportional to the square root of ε_{ss} (see Fig. S4(a) in the supplementary material[62]). Below $\varepsilon_{ss}/k_B = 28$ K, the h_0 value sharply decreases with increasing ε_{ss} because the open state is effectively stabilized by the enhancement of $\Delta\Omega$. Then, above $\varepsilon_{ss}/k_B = 28$ K, the h_0 value starts to increase because the destabilization of the open state by the increase in ΔF^{host} becomes significant. On the other hand, the border between areas (ii) and (iii) is almost constant at $h_0/\sigma_{ff} = 1.70$. This is because, at $P/P_0 = 1$, adsorption of guest molecules in the framework begins when the interlayer width h/σ_{ff} reaches ca. 1.75, which is slightly larger than the initial interlayer width of $h_0/\sigma_{ff} = 1.70$, with almost no dependence on ε_{ss}. These facts suggest that the gating behavior can be controlled by tuning the length of the pillars rather than enhancing the inter-framework and guest–framework interactions.

Our model is remindful of the Surface Force Apparatus (SFA) experiments[67,68] and molecular simulations for reproducing the experimental results,[69–71] which show oscillation of the solvation force due to the formation of stable layers of adsorbed molecules upon squeezing the two substrates. In the case of our models with the structural parameters discussed in this section, a monolayer is only formed between the solid layers at $P/P_0 < 1$, but more than two adsorbed layers should be inserted when larger chemical potential is imposed on the system. Actually, the real stacked-layer PCP, ELM-11, shows first gating transition by CO_2 adsorption at 0.2–0.3 bar and 273 K, followed by second gating transition at 6–9 bar,[72] though the structure of the adsorbed CO_2 in ELM-11 is somewhat different from that in our simple pore model.

D. Parameter sets for filling and gating behavior

The gating behavior of the models with $h_0/\sigma_{ff} > 2.1$ was also examined. Here, we take the model with $h_0/\sigma_{ff} = 2.70$ and $\varepsilon_{ss}/k_B = 28$ K as an example. Figure 8(a) shows the relative free energies $\Delta\Omega^{OS}$, $\Delta\Omega$, and ΔF^{host} of the model at the equilibrium transition pressure ($P/P_0 = 0.099$) as a function of the interlayer width. The interlayer width of the model in the degassed state (Fig. 8(b)) is about 1.7 times wider to accommodate the single layer of guest molecules. Therefore, after the filling with guest molecules is complete, the interlayer width shrinks to $h/\sigma_{ff} = 2.62$ because of the attractive forces from the guest molecules acting on the frameworks (filling state, see Fig. 8(c)), although ΔF^{host} increases because of the repulsion forces acting between the pillars and the solid layers. The interlayer width contracts continuously without any activation processes. Then, another stable state of $\Delta\Omega^{OS}$ appears at $h/\sigma_{ff} = 2.92$ with the formation of an ordered bilayer of guest molecules (open state, see Fig. 8(d)). An energy barrier in $\Delta\Omega^{OS}$ arises at $h/\sigma_{ff} = 2.78$ between the filling state and the open state, which is attributed not to ΔF^{host} but to $\Delta\Omega$, unlike the models showing one-step gating. The energy barrier E_A^{eq} is larger than $6\,k_B T/uc$; therefore, the equilibrium transition from the filling state to the open state should not occur according to the kinetics. However, the energy barrier decreases to $6\,k_B T/uc$ with an increase in the relative pressure to 0.123 (Fig. 8(e)). Namely, a spontaneous gate-opening transition from the filling state to the open state should be observed. Then, as also shown in Fig. 8(e), the backward gate-closing transition should occur at $P/P_0 = 0.094$. The resulting adsorption isotherm for the model with $h_0/\sigma_{ff} = 2.70$ is depicted in Fig. 8(f). The gradual step in the adsorption isotherm

around $P/P_0 = 0.08$ is due to filling of guest molecules with accompanying shrinkage of the interlayer width. The second uptake with the hysteresis comes from the gate-opening and -closing transitions. The filling and gating behavior obtained in our study should be analogous to that observed in ELM-12.[26] It is also worth noting that Bousquet *et al.*[61] have found similar shrinking and expanding transition behavior for the simple model of MIL-53, in which the *np* state is more stable than the *lp* state at the degassed state and the molecular size of the guest is smaller than the pore size of the *np* state (Case A1 in Sec. III A). However, our model is different from their model in that the Helmholtz free energy of the host only has a single minimum, which should be typical for stacked-layer PCPs.

The parameter sets of h_0 and ε_{ss} that generate the filling and gating behavior were explored, and the results are shown in Fig. 7(a). We categorized the parameter sets into three types: (vi), (vii), and (viii). The global minimum can switch from the filling state to the open state in areas (vi), (vii), and (viii) below $P/P_0 = 1$. That is, a two-step adsorption isotherm due to filling and gating is obtained in these three areas according to the theory of equilibrium. On the other hand, according to the kinetics, E_A^{eq} is always larger than $6\,k_B T$/uc in area (vi); therefore, the structural transition from the filling state to the open state does not occur. In area (vii), E_A^{op} and E_A^{cl} can become smaller than $6\,k_B T$/uc; it follows that the gate-opening and -closing transitions are observed according to the kinetics below $P/P_0 = 1$. Then, in area (viii), even E_A^{eq} can be less than $6\,k_B T$/uc, which yields a reversible two-step adsorption isotherm. The borders between the three areas depend little on ε_{ss} but strongly on h_0. This indicates that the filling and gating behavior can be controlled by tuning the length of the pillars rather than enhancing the inter-framework and guest–framework interactions, as in the one-step gating behavior.

E. Double gating behavior of spring-added model

We also investigated a model showing double gating behavior, which is a combination of the first-order shrinking and expanding transitions of the framework. In the model described above, the interlayer width contracts continuously during the filling process without any activation processes. Namely, the filling process is not the first-order transition, which should come from the high compressive stiffness of the host framework. We therefore estimated the elastic modulus of the model with $h_0/\sigma_{ff} = 2.70$ and $\varepsilon_{ss}/k_B = 28$ K by calculating a stress–strain curve and assuming a linear relation up to 4% strain. The obtained compressive and tensile moduli of the framework were 2.0 GPa and 0.37 GPa, respectively. The compressive stiffness is one order of magnitude higher than the tensile stiffness because of the repulsion forces acting between the pillars and the solid layers. This high stiffness for compression prevents a large shrinkage of the host framework, so the first-order transition, which requires a dramatic change in the interlayer width, cannot be achieved. Therefore, to control the compressive stiffness of the host framework, we added a harmonic spring on top of the pillars in our model. The height of the pillars was set so that the initial interlayer width h_0/σ_{ff} of the model without the harmonic springs was 2.40. The equilibrium length of the harmonic spring was determined so that the resulting initial interlayer width became 2.70. Then, the force constant of the harmonic spring was adjusted so that the compressive elastic modulus of the framework, E_{comp}, was 0.76 GPa. The E_{comp} value set in the spring-added model is less than half that of the model with $h_0/\sigma_{ff} = 2.70$ and $\varepsilon_{ss}/k_B = 28$ K without the harmonic springs.

The relative free energies $\Delta\Omega^{OS}$, $\Delta\Omega$, and ΔF^{host} of the spring-added model at $P/P_0 = 0.066$ are depicted in Fig. 9(a). The obtained $\Delta\Omega^{OS}$ has two minima at $h/\sigma_{ff} = 2.64$ and $h/\sigma_{ff} = 2.46$, and the system is in a bistable state. The system
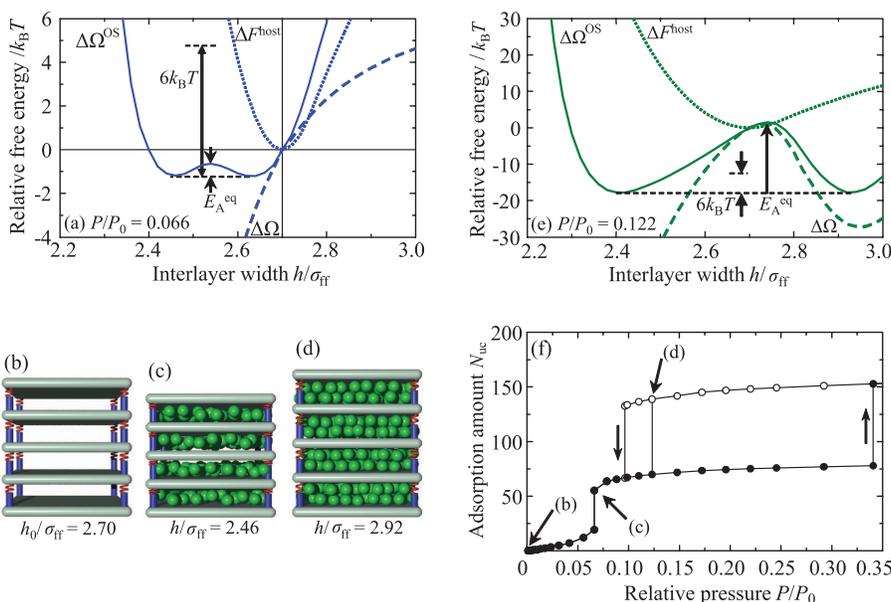
FIG. 9. (a) Relative free energies $\Delta\Omega^{OS}$, $\Delta\Omega$, and ΔF^{host} for spring-added model with $h_0/\sigma_{ff} = 2.70$ and $\varepsilon_{ss}/k_B = 28$ K as a function of interlayer width at $P/P_0 = 0.066$; snapshots of the system: (b) $h_0/\sigma_{ff} = 2.70$ and $P/P_0 = 0$; (c) $h/\sigma_{ff} = 2.46$ and $P/P_0 = 0.066$, and (d) $h/\sigma_{ff} = 2.92$ and $P/P_0 = 0.122$; (e) relative osmotic free energies at $P/P_0 = 0.122$; (f) resulting adsorption isotherm.

continuously shifts from the degassed state of $h_0/\sigma_{ff} = 2.70$ (Fig. 9(b)) to the state of $h/\sigma_{ff} = 2.64$ owing to filling of the guest molecules. An energy barrier in $\Delta\Omega^{OS}$ between the minima is smaller than $6\,k_BT/\text{uc}$. Therefore, the first-order transition from the interlayer width of $h/\sigma_{ff} = 2.64$ to that of $h/\sigma_{ff} = 2.46$ (Fig. 9(c)), namely a shrinking transition, should be observed. Then, another bistable state appears at $P/P_0 = 0.122$ (Fig. 9(e)). One stable state at $h/\sigma_{ff} = 2.42$ accommodates a single layer of guest molecules, and the other one at $h/\sigma_{ff} = 2.92$ (Fig. 9(d)) has an ordered bilayer of guest molecules. An energy barrier in $\Delta\Omega^{OS}$ between the minima is larger than $6\,k_BT/\text{uc}$; thus, the equilibrium transition from the narrower interlayer width to the wider one should not occur according to the kinetics. However, the energy barriers for the adsorption and desorption processes decrease to $6\,k_BT/\text{uc}$ at $P/P_0 = 0.34$ and $P/P_0 = 0.10$, respectively, which provides the second gating behavior with hysteresis. The resulting adsorption isotherm of the spring-added model with $h_0/\sigma_{ff} = 2.70$ is shown in Fig. 9(f). The isotherm suggests that the softening of the framework results in a steep uptake due to the shrinking transition and widening of the hysteresis loop arising from the second gate-opening and -closing transitions. The shrinking and expanding transitions, which are both first order and feature of the breathing phenomenon in MIL-53, have been reproduced with the simple model of MIL-53 by Bousquet *et al.* (Cases B1 and B2 in Sec. III A).[61] The Helmholtz free energy of the host for their model has double minima, and the *np* state is unstable compared with the *lp* state without the guest adsorption. On the other hand, our model exhibits the shrinking transition due to the stabilization only by the guest adsorption, though the Helmholtz free energy of the host has no minimum at the shrunk state ($h/\sigma_{ff} = 2.46$, Fig. 9(a)).

The dependence of the equilibrium structural transition pressure on the compressive elastic modulus was examined; the results are shown in Fig. 10. According to the theory of equilibrium, the double gating behavior is observed for the models with $E_{comp} < 0.83$ GPa. The enhancement of E_{comp} increases the resistance to shrinkage of the host framework; therefore, the shrinking transition pressure is increased. However, for $E_{comp} > 0.83$ GPa, the first-order shrinking transition vanishes; instead, the interlayer width contracts continuously without any activation processes ("filling transition"). On the other hand, in the expanding transition, the increase in the compressive stiffness helps the host framework expand,
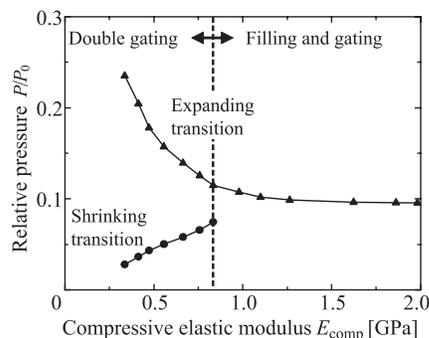
which decreases the expanding transition pressure. These results suggest that the gating behaviors (i.e., filling and gating and double gating) strongly depend on the length of the pillars and the stiffness of the host framework. Interestingly, the compressive moduli of our double gating models roughly agree with those of atomistic models of PCPs showing double gating obtained by *ab initio* quantum mechanical calculations: 0.90 GPa for MIL-53(Al) and 0.45 GPa for DMOF-1.[73]

IV. CONCLUSION

We investigated the dependence of the one-step gating and filling and gating behaviors of simplified stacked-layer PCP models on the initial interlayer width h_0 and the inter-framework interaction parameter ε_{ss} by conducting GCMC simulations and a free-energy analysis. The gating behavior can be transformed from one-step gating to filling and gating by increasing h_0 rather than changing ε_{ss}. This result can explain the difference between the gating behaviors of ELM-11[8] and ELM-12:[26] CO_2 adsorption on ELM-11, which is composed of BF_4^- pillars, shows one-step gating accompanied by a hysteresis loop, and ELM-12, with $CF_3SO_3^-$ pillars, which are larger than BF_4^-, shows filling and gating exhibiting a hysteresis loop on the second step.

We also studied the double gating behavior, which is a combination of the first-order shrinking and expanding transitions of the host framework. To reduce the compressive stiffness of the host framework, we cut the pillars and added virtual springs between the pillars and the solid layers of our simplified model. The softening of the host framework yielded the transformation from filling and gating to double gating behavior. The compressive moduli of our models showing the double gating behavior roughly agree with those of the atomistic models of PCPs obtained by *ab initio* quantum mechanical calculations for MIL-53(Al) and DMOF-1,[73] which proves the validity of our approach.

We believe that our results could serve as a guideline for controlling the gating pressure of PCPs by exchanging the chemical components.

FIG. 10. Dependence of equilibrium transition pressures on compressive elastic modulus of spring-added model.

[1] S. Kitagawa, R. Kitaura, and S. Noro, Angew. Chem. Int. Ed. **43**, 2334 (2004).
[2] J. L. C. Rowsell and O. M. Yaghi, Microporous Mesoporous Mater. **73**, 3 (2004).
[3] M. J. Rosseinsky, Microporous Mesoporous Mater. **73**, 15 (2004).
[4] S. Horike, S. Shimomura, and S. Kitagawa, Nat. Chem. **1**, 695 (2009).
[5] S. Takamizawa, E. Nakata, and H. Yokoyama, Inorg. Chem. Commun. **6**, 763 (2003).
[6] H. Kajiro, A. Kondo, K. Kaneko, and H. Kanoh, Int. J. Mol. Sci. **11**, 3803 (2010).

[7] H. Kanoh, A. Kondo, H. Noguchi, H. Kajiro, A. Tohdoh, Y. Hattori, W.-C. Xu, M. Inoue, T. Sugiura, K. Morita, H. Tanaka, T. Ohba, and K. Kaneko, J. Colloid Interface Sci. **334**, 1 (2009).

[8] A. Kondo, H. Noguchi, S. Ohnishi, H. Kajiro, A. Tohdoh, Y. Hattori, W.-C. Xu, H. Tanaka, H. Kanoh, and K. Kaneko, Nano Lett. **6**, 2581 (2006).

[9] K. Nakagawa, D. Tanaka, S. Horike, S. Shimomura, M. Higuchi, and S. Kitagawa, Chem. Commun. **46**, 4258 (2010).

[10] K. Uemura, S. Kitagawa, K. Fukui, and K. Saito, J. Am. Chem. Soc. **126**, 3817 (2004).

[11] R. Kitaura, K. Seki, G. Akiyama, and S. Kitagawa, Angew. Chem. Int. Ed. **42**, 428 (2003).

[12] K. Uemura, Y. Yamasaki, Y. Komagawa, K. Tanaka, and H. Kita, Angew. Chem. Int. Ed. **46**, 6662 (2007).

[13] K. Seki, Phys. Chem. Chem. Phys. **4**, 1968 (2002).

[14] K. Uemura, F. Onishi, Y. Yamasaki, and H. Kita, J. Solid State Chem. **182**, 2852 (2009).

[15] J. P. S. Mowat, V. R. Seymour, J. M. Griffin, S. P. Thompson, A. M. Z. Slawin, D. Fairen-Jimenez, T. Duren, S. E. Ashbrook, and P. A. Wright, Dalton Trans. **41**, 3937 (2012).

[16] C. Volkringer, T. Loiseau, N. Guillou, G. Ferey, E. Elkaim, and A. Vimont, Dalton Trans. **2009**, 2241.

[17] G. Chaplais, A. Simon-Masseron, F. Porcher, C. Lecomte, D. Bazer-Bachi, N. Bats, and J. Patarin, Phys. Chem. Chem. Phys. **11**, 5241 (2009).

[18] F. Millange, N. Guillou, R. I. Walton, J.-M. Greneche, I. Margiolaki, and G. Ferey, Chem. Commun. **2008**, 4732.

[19] S. Bourrelly, P. L. Llewellyn, C. Serre, F. Millange, T. Loiseau, and G. Férey, J. Am. Chem. Soc. **127**, 13519 (2005).

[20] C. Serre, F. Millange, C. Thouvenot, M. Nogues, G. Marsolier, D. Louer, and G. Ferey, J. Am. Chem. Soc. **124**, 13519 (2002).

[21] T. Duren, L. Sarkisov, O. M. Yaghi, and R. Q. Snurr, Langmuir **20**, 2683 (2004).

[22] N. Yanai, K. Kitayama, Y. Hijikata, H. Sato, R. Matsuda, Y. Kubota, M. Takata, M. Mizuno, T. Uemura, and S. Kitagawa, Nat. Mater. **10**, 787 (2011).

[23] T. Loiseau, C. Serre, C. Huguenard, G. Fink, F. Taulelle, M. Henry, T. Bataille, and G. Férey, Chem. Eur. J **10**, 1373 (2004).

[24] S. Couck, J. F. M. Denayer, G. V. Baron, T. Rémy, J. Gascon, and F. Kapteijn, J. Am. Chem. Soc. **131**, 6326 (2009).

[25] S. Henke, A. Schneemann, A. Wütscher, and R. A. Fischer, J. Am. Chem. Soc. **134**, 9464 (2012).

[26] A. Kondo, H. Noguchi, L. Carlucci, D. M. Proserpio, G. Ciani, H. Kajiro, T. Ohba, H. Kanoh, and K. Kaneko, J. Am. Chem. Soc. **129**, 12362 (2007).

[27] T. Devic, F. Salles, S. Bourrelly, B. Moulin, G. Maurin, P. Horcajada, C. Serre, A. Vimont, J.-C. Lavalley, H. Leclerc, G. Clet, M. Daturi, P. L. Llewellyn, Y. Filinchuk, and G. Ferey, J. Mater. Chem. **22**, 10266 (2012).

[28] T. Fukushima, S. Horike, H. Kobayashi, M. Tsujimoto, S. Isoda, M. L. Foo, Y. Kubota, M. Takata, and S. Kitagawa, J. Am. Chem. Soc. **134**, 13341 (2012).

[29] T. Fukushima, S. Horike, Y. Inubushi, K. Nakagawa, Y. Kubota, M. Takata, and S. Kitagawa, Angew. Chem. Int. Ed. **49**, 4820 (2010).

[30] Y. Sakata, S. Furukawa, C. Kim, and S. Kitagawa, Chem. Lett. **41**, 1436 (2012).

[31] D. Tanaka, A. Henke, K. Albrecht, M. Moeller, K. Nakagawa, S. Kitagawa, and J. Groll, Nature Chem. **2**, 410 (2010).

[32] R. Babarao and J. Jiang, J. Am. Chem. Soc. **131**, 11417 (2009).

[33] D. H. Jung, D. Kim, T. B. Lee, S. B. Choi, J. H. Yoon, J. Kim, K. Choi, and S.-H. Choi, J. Phys. Chem. B **110**, 22987 (2006).

[34] Q. Yang and C. Zhong, J. Phys. Chem. B **109**, 11862 (2005).

[35] L. Sarkisov, T. Duren, and R. Q. Snurr, Mol. Phys. **102**, 211 (2004).

[36] A. Vishnyakov, P. I. Ravikovitch, A. V. Neimark, M. Bülow, and Q. M. Wang, Nano Lett. **3**, 713 (2003).

[37] R. Babarao, J. Jiang, and S. I. Sandler, Langmuir **25**, 5239 (2009).

[38] J. R. Karra and K. S. Walton, J. Phys. Chem. C **114**, 15735 (2010).

[39] R. Babarao, M. Eddaoudi, and J. W. Jiang, Langmuir **26**, 11196 (2010).

[40] Q. Yang, C. Xue, C. Zhong, and J.-F. Chen, AIChE J. **53**, 2832 (2007).

[41] R. Babarao, Z. Hu, J. Jiang, S. Chempath, and S. I. Sandler, Langmuir **23**, 659 (2007).

[42] Q. Yang and C. Zhong, ChemPhysChem **7**, 1417 (2006).

[43] R. Babarao and J. Jiang, Langmuir **24**, 5474 (2008).

[44] A. I. Skoulidas, J. Am. Chem. Soc. **126**, 1356 (2004).

[45] C. E. Wilmer, M. Leaf, C. Y. Lee, O. K. Farha, B. G. Hauser, J. T. Hupp, and R. Q. Snurr, Nat. Chem. **4**, 83 (2012).

[46] T. Watanabe and D. S. Sholl, Langmuir **28**, 14114 (2012).

[47] D. Dubbeldam, R. Krishna, and R. Q. Snurr, J. Phys. Chem. C **113**, 19317 (2009).

[48] J. A. Greathouse and M. D. Allendorf, J. Phys. Chem. C **112**, 5795 (2008).

[49] B. L. Huang, A. J. H. Mcgaughey, and M. Kaviany, Int. J. Heat Mass Transfer **50**, 393 (2007).

[50] S. Amirjalayer and R. Schmid, J. Phys. Chem. C **112**, 14980 (2008).

[51] S. Amirjalayer, M. Tafipolsky, and R. Schmid, Angew. Chem. Int. Ed. **46**, 463 (2007).

[52] A. Ghoufi, G. Maurin, and G. Ferey, J. Phys, Chem. Lett. **1**, 2810 (2010).

[53] A. Ghoufi and G. Maurin, J. Phys. Chem. C **114**, 6496 (2010).

[54] F. Salles, A. Ghoufi, G. Maurin, R. G. Bell, C. Mellot-Draznieks, and G. Ferey, Angew. Chem. Int. Ed. **47**, 8487 (2008).

[55] C. Triguero, F.-X. Coudert, A. Boutin, A. H. Fuchs, and A. V. Neimark, J. Chem. Phys. **137**, 184702 (2012).

[56] C. Triguero, F.-X. Coudert, A. Boutin, A. H. Fuchs, and A. V. Neimark, J. Phys. Chem. Lett. **2**, 2033 (2011).

[57] H. Sugiyama, S. Watanabe, H. Tanaka, and M. T. Miyahara, Langmuir **28**, 5093 (2012).

[58] S. Watanabe, H. Sugiyama, H. Adachi, H. Tanaka, and M. T. Miyahara, J. Chem. Phys. **130**, 164707 (2009).

[59] R. Numaguchi, H. Tanaka, S. Watanabe, and M. T. Miyahara, J. Chem. Phys. **138**, 054708 (2013).

[60] D. Bousquet, F.-X. Coudert, and A. Boutin, J. Chem. Phys. **137**, 044118 (2012).

[61] D. Bousquet, F.-X. Coudert, A. G. J. Fossati, A. V. Neimark, A. H. Fuchs, and A. Boutin, J. Chem. Phys. **138**, 174706 (2013).

[62] See supplementary material at http://dx.doi.org/10.1063/1.4862735 for details on intra-framework potential energy, osmotic free energy, and dependence of the grand free energy on solid-solid interaction parameter.

[63] J. K. Johnson, J. A. Zollweg, and K. E. Gubbins, Mol. Phys. **78**, 591 (1993).

[64] A. Lotfi, J. Vrabec, and J. Fischer, Mol. Phys. **76**, 1319 (1992).

[65] F.-X. Coudert, M. Jeffroy, A. H. Fuchs, A. Boutin, and C. Mellot-Draznieks, J. Am. Chem. Soc. **130**, 14294 (2008).

[66] B. K. Peterson and K. E. Gubbins, Mol. Phys. **62**, 215 (1987).

[67] R. M. Pashley and J. N. Israelachvili, J. Colloid Interface Sci. **101**, 511 (1984).

[68] R. G. Horn and J. N. Israelachvili, Chem. Phys. Lett. **71**, 192 (1980).

[69] I. K. Snook and W. V. Megen, J. Chem. Phys. **72**, 2907 (1980).

[70] M. Schoen, S. Hess, and D. J. Diestler, Phys. Rev. E **52**, 2587 (1995).

[71] P. B. Balbuena, D. Berry, and K. E. Gubbins, J. Phys. Chem. **97**, 937 (1993).

[72] J. Yang, Q. Yu, Q. Zhao, J. Liang, J. Dong, and J. Li, Microporous Mesoporous Mater. **161**, 154 (2012).

[73] A. U. Ortiz, A. Boutin, A. H. Fuchs, and F.-X. Coudert, Phys. Rev. Lett. **109**, 195502 (2012).